Preparation and chemical characterization of neodymium-doped molybdenum oxide films grown using spray pyrolysis

J. E. Alfonso[a,*], and L. C. Moreno[b]
[a]*Grupo de Ciencia Materiales y superficies, Departamento de Física, Universidad Nacional de Colombia, AA 5997 Bogotá DC, Colombia*
[b]*Departamento de Química, Universidad Nacional de Colombia, AA 5997 Bogotá DC, Colombia*
[*]*Tel: +57-1-3165000 ext. 13040, e-mail: jealfonsoo@unal.edu.co*

Received 17 September 2013; accepted 9 December 2013

We studied the crystallinity, morphology, and surface composition of Nd-doped molybdenum oxide films grown on glass slides through spray pyrolysis. After fabrication, the films were subjected to thermal treatment in oxygen for periods ranging from 2 to 20 hours. The films were structurally characterized through X-ray diffraction (XRD), their bulk chemical composition was determined using Energy-Dispersive X-ray analysis (EDX), and their surface composition was determined using X-ray Photoelectron Spectroscopy (XPS). The XRD results show that the films obtained from different dissolution volumes and at substrate temperature of 300° C exhibit the characteristics of the oxygen-deficient molybdenum trioxide Mo_9O_{26} phase. The films subjected to different thermal treatments exhibit a mixture of Mo_9O_{26} and $Mo_{17}O_{47}$ phases. EDX study shows the energy belonging to the L line of Nd. Finally, films doped with Nd and subjected to a thermal treatment of 20h were analyzed through XPS, showing the binding energies at the crystalline lattice correspond to Nd_2 $(MoO_4)_3$ and $Nd_2Mo_2O_7$.

Keywords: Thin films; spray pyrolysis; molybdenum oxide; morphology.

PACS: 34.50.D; 61.10.N; 33.60

1. Introduction

Molybdenum trioxide is a transition metal oxide with optical properties such as photochromism, which allows applications such as display manufacture, optical smart windows, and high-density memory devices [1-4]. In addition, the incorporation of ions such as Li into the crystalline structure of the molybdenum oxide has allowed the manufacture of batteries in which the molybdenum oxide acts as a cathode [5-7], and in recent years Jinshu Wang *et al.* [8] studied the emission property of new kinds of rare-earth oxide-molybdenum cermet cathodes constructed using powder metallurgy. Wang showed that adding either single rare-earth oxides La_2O_3, Y_2O_3, and Gd_2O_3 or a mixture of these rare-earth oxides into molybdenum oxide can improve the secondary emission coefficient of the cathode, and recently Alfonso *et al.* [9] evaluated the thermal expansion coefficient of MoO_3 doped with Nd. Additionally, some research has concluded that MoO_3 improves the sensitivity of the detection of gases such as NH_3 when coated with Ti thin films [10] and CO when doped with SnO_2 nanoparticles [11].

The previous applications can be explained by the crystalline structures in which MoO_3 grows, *i.e.*, α-MoO_3 andβ-MoO_3. The former is orthorhombic, formed by MoO_6 octahedral chains that share edges with two similar chains and form the stoichiometric MoO_3. These layers are stacked in a staggered arrangement and are held together by weak Van der Waals forces. β-MoO_3 has a monocyclic structure. It has a ReO3-type structure in which MoO_6 octahedra share only the corners with each other and can be seen as an infinite thin chain of MoO_6 octahedra with shared edges [12]. These octahedra are extended tunnels that can be used as conduits and intercalation sites for mobile ions. Taking advantage of the crystal structure and considering the great technological interest that has arisen from inserting rare-earth ions into the molybdenum oxide structure, due their greater chemical and thermal stability, which may improve the optical and magnetic properties of the Nd ion, in the present paper we grew films of Nd-doped molybdenum oxides through the spray pyrolysis method.

2. Experimental Details

$Nd_xMo_{1-x}O_3$ thin films were prepared from solutions in water of ammonium molybdate tetrahydrate (NH_4) $6Mo_7O_{24}4H_2O$ Merck analytical reactive, (0.1 M) and neodymium nitrate (0.1 M) via the spray pyrolysis method. These solutions were atomized on glass substrates heated at 300° C, and as the transport gas air at 2.0 atm pressure (2.026×10^5 Pa) was used. The thickness of the films was varied by atomizing the volumes of dissolution between 5.0 and 20.0 mL, and reached values between 250 nm to 1μ. The Mo^{6+} and Nd^{3+} cation concentration in the atomized dissolution was 0.1 M (Mo^{6+} 0.095 M and Nd^{3+} 0.05 M).

In order to investigate the influence of heat treatment and insertion of the Nd^{3+} ion on the crystallographic structure of the molybdenum oxide films, they were heated from two to twenty hours in a furnace with a heating slope of 5° C/min up to 500° C and under an oxygen flow of 4 mL/min. The final films have a good adherence and reflect a blue which varied

of pale, in films heated for 2 h, to intense in films heated for 20 h.

The X-ray diffraction (XRD) patterns were taken with a Panalytical X-pert Pro MPD diffractometer working at 45 kV and 40 mA, using Cu Kα radiation, in steps of 0.2 degrees. The X-ray diffraction patterns were analyzed using the DRXWIN software. Studies of the chemical composition of the films were done by the microsonde of the electron microscope Quanta FEI 200, working at an electron acceleration voltage of 20 kV. The surface chemical composition was determined through X-ray photoelectron spectroscopy (XPS) using a Leybold-Heraeus LHS-10 spectrometer under a vacuum higher than 3×10^{-8} Pa using Mg Kα radiation (1254.6 eV) and a constant pass energy of 20 eV. Binding energies were referred to the C1s line (284.6 eV) of the adventitious contamination layer.

3. Results and Discussion

Figure 1 shows the XRD patterns recorded from the samples that were grown using different volumes of dissolution containing ammonium molybdate tetra-hydrate ($(NH_3)_6Mo_7O_{24}.4H_2O$) and neodymium nitrate with an atomic percentage of 5% of Nd, while the substrate temperature was kept at 300° C. In general, the XRD patterns are composed of very broad lines, indicating that the samples have a poor crystalline character. However, superposed on those broad bands, a few sharper lines are clearly visible, which could be associated with the presence of the triclinic Mo_9O_{26} phases (pdf chart 05-0441), which can be considered oxygen-deficient variants of the MoO_3 stoichiometric phase. From those patterns, it is difficult to discern significant intensity variations of the different diffraction lines.

In order to investigate the effect that thermal treatment has on the crystallographic structure of the neodymium-doped molybdenum oxide films, they were subjected to different thermal treatments. Thus, samples prepared with 10 mL of dissolution of $(NH_3)_6Mo_7O_{24}.4H_2O$ and at 5% Nd were heated, initially for 2h, and after that the same films were heated for 20 h in a controlled oxygen atmospheres at 500° C. It is important to note that a pure molybdenum oxide sample (not neodymium-doped) was introduced into the furnace, in order to establish if is produced change structural in the films doped.

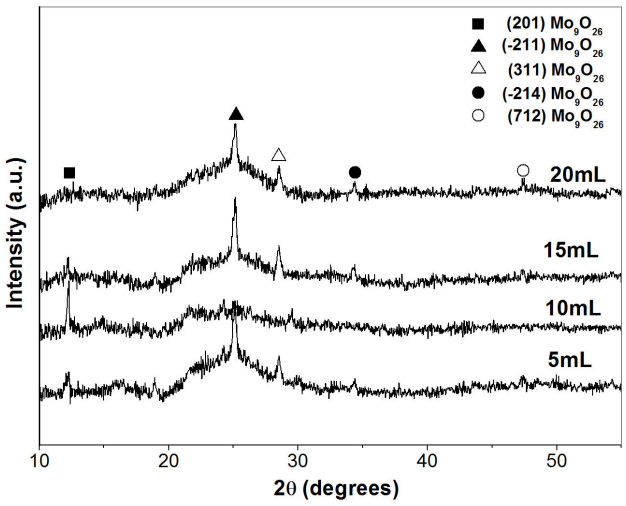

FIGURE 1. XRD pattern of neodymium-doped molybdenum oxide films at different volumes of dissolution.

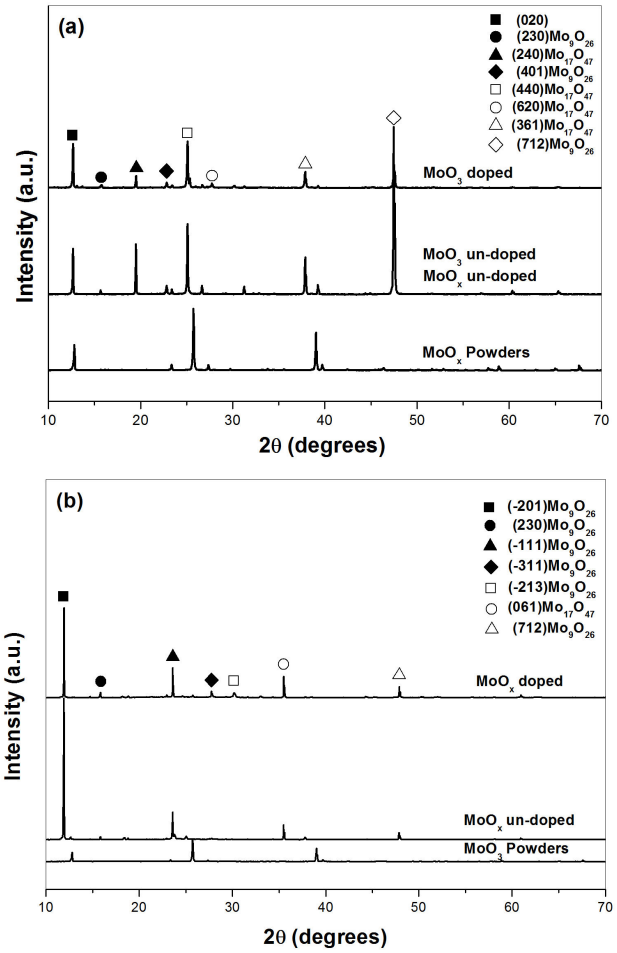

FIGURE 2. XRD patterns of the Molybdenum oxide films prepared using spray pyrolysis a) thermal treatment 2 h in oxygen, and b) thermal treatment 20 h in oxygen. α-MoO_3 powder appears as a reference.

The XRD patterns recorded from the materials resulting from these thermal treatments are shown in Figs. 2a and 2b. Figure 2a allowed determining that the Nd-doped samples treated for 2 h periods display crystallographic behavior similar to the films grown without Nd, since both films showed the (020) plane of the MoO_3 (PDF 350609) (230), (401) and (712) planes of the monoclinic Mo_9O_{26} phase. Additionally, the two films show (240), (440), (620), and (361) planes associated with the orthorhombic $Mo_{17}O_{47}$ phase (PDF7130345). In the XRD pattern associated with the Nd-doped film, there is no presence of planes associated with molybdates or neodymium oxides. Also, it is important

to indicate that the ratio of the (712) plane intensities of the non-doped film and the doped one was two to one.

The previous results indicate that the molybdenum oxide films without doping have two crystallographic phases, the monoclinic Mo_9O_{26} (a=16.74Å, b=4.01 Å, c=14.53 Å) and the orthorhombic $Mo_{17}O_{47}$ (a=21.61Å, b=19.63 Å, c=3.95 Å); the monoclinic phase grew with preferential growth along the (712) plane of monoclinic phase. The films to which Nd was added have a lower intensity of the X-ray diffraction, almost half the intensity of the un-doped films, which could indicate that they likely have incorporated Nd into the crystalline lattice of the molybdenum oxides present in the film.

The XRD pattern of the films annealed in oxygen atmospheres for 20 h (Fig. 2b) allowed determining that the orthorhombic phase of the un-doped molybdenum oxide film, with previous heat treatment, decreased substantially, and in its place the monoclinic Mo_9O_{26} phase growth appeared, with a high degree of texture throughout plane (-201). Other planes associated with the same phase are: (230), (-111), (-311), (-213), and (712). Additionally, the (610) plane of the $Mo_{17}O_{47}$ phase appears. The film grown with doping (Fig. 2b) reproduces the crystallographic behavior of the film without Nd, except for the values of intensity, since the intensity of plane (-201) is 1.5 times higher with respect to the same plane of the Nd-doped film. The results obtained suggest that films treated thermally for 20 h have a transitional crystallographic phase with respect to those treated for 2 h. The orthorhombic phase is transformed, at a high percentage, into the monoclinic phase, and the formation of $Mo_{17}O_{47}$ phase maybe can be explained, if we considered that the rate of loss the oxygen of the lattice of the molybdenum oxide, due the thermal treatment in the interphase substrate-film, is

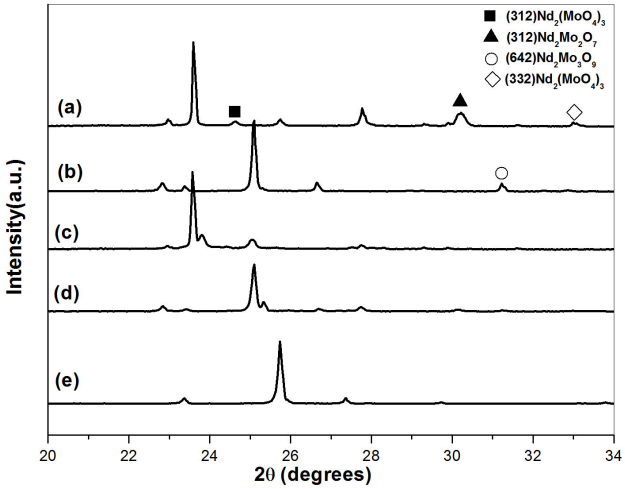

FIGURE 3. (a) XRD pattern of neodymium-doped molybdenum oxide films with thermal treatment of 20 h; (b) XRD pattern of neodymium-doped molybdenum oxide films with thermal treatment of 2 h; (c) XRD pattern of un-doped and molybdenum oxide film, thermal treatment of 20 h; (d) XRD pattern of un-doped molybdenum oxide film with thermal treatment of 2 h; (e) XRD pattern of MoO_3 powders.

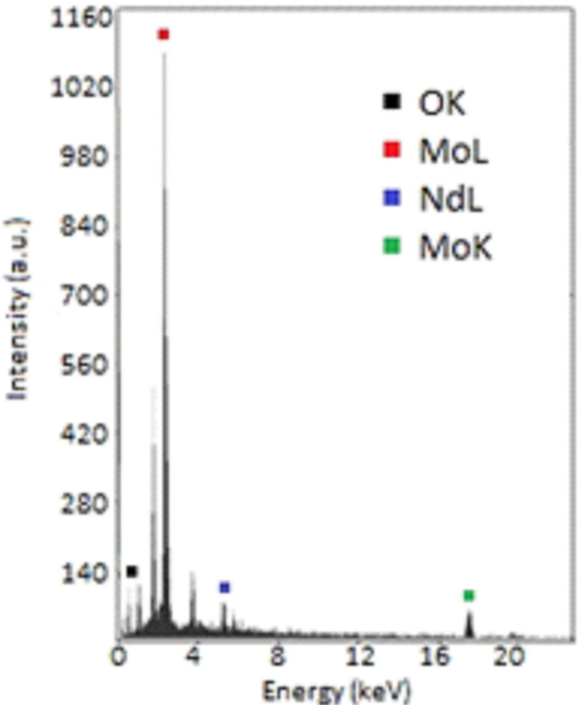

FIGURE 4. EDX pattern of the molybdenum oxide film doped with Nd and with thermal treatment for 20 hs in oxygen.

is higher that the rate of incorporation of oxygen used in annealing of the film.

Moreover, in order to observe low intensity planes, Fig. 3 was constructed, where it is possible to observe XRD patterns between 20° and 34° of the doped and un-doped films with thermal treatment of 2 and 20 h. Fig. 3a shows three planes not identified previously in Fig. 2b. These planes are at 24.61° and 33.00°, belonging to the (312) and (332) planes of the monoclinic crystallographic phase of $Nd_2(MoO_4)_3$ (PDF 251174). The most intense plane is located at 30.19°, belonging to the (312) plane of the orthorhombic crystallographic phase of $Nd_2Mo_2O_7$ (PDF 350253). Figure 3b shows the (642) plane at 31.2°, belonging to $Nd_2Mo_3O_9$ (PDF 350247) of the tetragonal crystallographic phase. These results allowed establishing that the MoO_3 films incorporated Nd into

TABLE I. Average concentration of elements (at %) in films of molybdenum oxide doped with Nd.

Film	Mo	O	Nd	Mo/Nd
MoO_3:Nd				
without heat treatment	25.08	73.90	1.52	16.50
MoO_3:Nd				
with 2-h heat treatment	32.86	65.12	2.02	16.27
MoO_3:Nd				
with 20-h heat treatment	28.50	69.18	2.32	12.28
Theoretical				
composition	24.20	74.52	1.27	19.06

their crystallographic lattice, since new compounds associated with molybdanates appear.

Figure 4 shows the results of EDX analysis done on the film in Fig. 3d. In the energy spectrum OK_α and Nd L_α, MoL_α lines can be seen. Average Nd values in the doped films are shown in Table I.

On the basis of the compounds used in the preparation of the films, and taking into account the electro- neutrality of Mo^{+6} and Nd^{3+}, we found that the most probable chemical formula for the theoretical elemental composition shown in Table I is $Mo_{0.95}Nd_{0.05}O_{2.925}$. Moreover, on the basis of the relationship between the percentage of atoms of Mo/ Nd, and taking into account XRD results, we can establish that it is most likely that in all cases Nd was incorporated to the crystallographic lattice of the molybdenum oxides and that the decrease of the Mo/Nd relation upon increasing the time of heat treatment may indicate sublimation of the molybdenum.

An XPS analysis was carried out on doped (5% Nd) and un-doped molybdenum oxide films with a thermal treatment of 20 h. The results obtained are shown in Fig. 5 a-d. Figures 5a and 5b show XPS spectra taken of un-doped molybdenum oxide films and those doped with Nd. In the spectra, Mo 3d spin-orbit doublets of the un-doped and doped films can be observed. The binding energies of Mo 3d photoelectron peaks are centered at 232.4 eV ($3d_{5/2}$) and 235.5 eV ($3d_{3/2}$) in the un-doped Mo_{Ox} films. These values of the binding energy are associated with the oxidation state Mo^{+6} of Mo [13]. Figure 5c shows the XPS spectrum of the binding energies of O 1s, with the peak centered at 530.5 eV belonging to the binding of Mo-O in MoO_3 [14]. These results suggest that the surface of the Mo_6O_{29} films reacts chemically with oxygen from the atmosphere to form the MoO_3 phase.

The XPS spectra of the doped films was more complex, since the experimental spectrum was adjusted with Mo 3d spin-orbit doublets centered at 230.1 eV, 231.6 eV, and 233.0 eV, belonging to Mo $3d_{5/2}$. These binding energies correspond to the Mo^{+4}, Mo^{+5}, and Mo^{+6} oxidation states of Mo, which were reported by Sunu *et al.* [15].

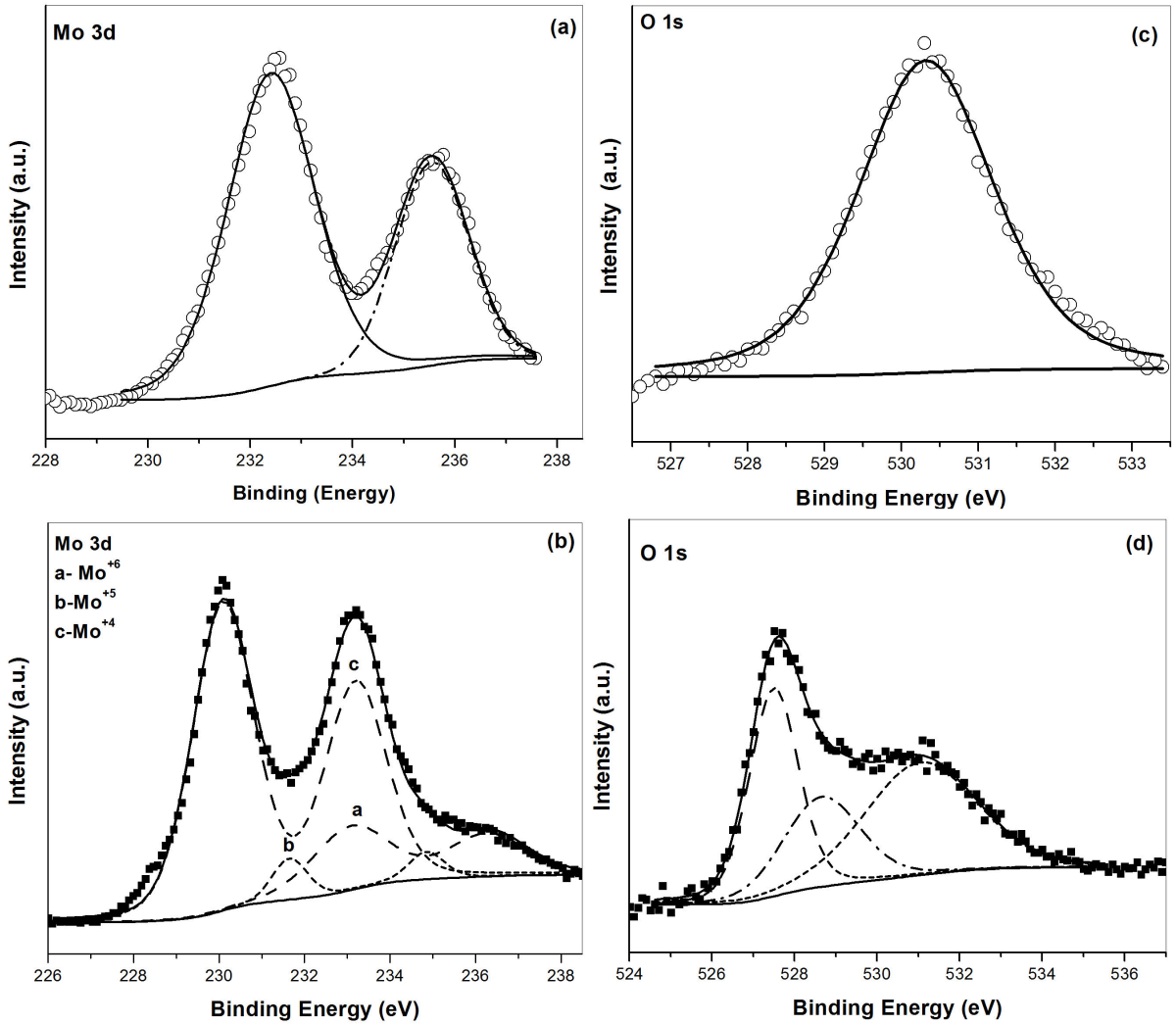

FIGURE 5. a) XPS spectra of Mo 3d on MoO_x, b) XPS spectra Mo 3d on MoO_x doped with Nd, c) XPS spectra of O 1s on MoO_x, d) XPS spectra of O 1s on MoO_x doped with Nd.

Figure 5d shows the XPS spectrum of the binding energy of O 1s. This spectrum is formed by three peaks, the first centered at 527.5 eV, which corresponds to the binding O-Mo (Mo^{+4}), the second centered at 528.6 eV, which corresponds to the binding O-Mo (Mo^{+5}), and the third centered at 531.1 eV, which corresponds to the binding O-Mo(Mo^{+6})

The XPS results are in agreement with the XRD, since the presence of energies associated with Mo^{+4} and Mo^{+6} oxidation states could be explained by the formation of $Nd_2Mo_2O_7$ and $Nd_2(MoO_4)_3$ compounds, where Mo has these valences states. The oxidation state Mo^{+5} can be explain if the results of the EDX are considered, where the Mo/Nd relation had the lower value, which indicated that the Molybdenum was sublimated. These results are in agreement with those obtained by Xingyi *et al*., who reported that the partial reduction of Mo^{+6} to Mo^{+5} is accompanied by the loss of Mo [17]

4. Conclusions

In this paper we grew films of various oxides of molybdenum doped with Nd through the spray pyrolysis method under different thermodynamic conditions and assessed their crystallographic behavior and surface chemical composition. Basically, it was established that moderate thermal treatments produced films with orthorhombic and monoclinic structures ($Mo_{17}O_{47}$, Mo_9O_{26}), which are the oxygen-deficient phase of MoO_3, and prolonged thermal treatment predominantly produced films with a monoclinic structure and with the presence of $Nd_2(MoO_4)_3$ and $Nd_2Mo_2O_7$ compounds.

Additionally, we established that in these films the binding energy of molybdenum corresponds to Mo with valence states of +6, +5, and +4. The importance of this research lies in the fact that for the first time, results of molybdenum oxides films doped with Nd are shown, which involves new possibilities for the development optical devices.

Acknowledgements

The authors gratefully acknowledge the financial support of the Research Division of "Universidad Nacional de Colombia (DIB)", and thank professors Jose Marco for the XPS measurements and Julio Evelio Rodriguez for the collaboration with the thermal treatments.

1. A. Abdellaoui, L. Martin, and A. Donnadieu, *Phys. Status Solidi A* **109** (1988) 455.
2. M.A. Quevedo-Lopez, R. F. Reidy, R. A. Orozco-Teran, O. Mendoza-Gonzalez, and R. Ramirez-Bon, *J. Mater. Sci. Mater. Electron* **11** (2000) 151.
3. C. G. Granqvist, *Solid State Ionics* **53–56** (1992) 479.
4. A. M. Anderson, C.G. Granquvist, and J.R. Stevens, *Appl. Opt.* **28** (1989) 3295.
5. G. Guzman, B. Yebka, J. Livage, and C. Julien, *Solid state Ionics* **86-88** (1996) 407.
6. C. Julien, G.A. Nazri, J.P. Guesdon, A. Gorenstein, A. Khelfa, and O.M. Hussain, *Solid State Ionics* **73** (1994) 319.
7. M. Hashimoto, S. Watanuki, N. Koshida, M. Komuro, and N. Atoda, *J. Appl. Phys., Part I* **35** (1996) 3665.
8. Jinshu Wang, Hongyi Li, Sa Yang, Yanqin Liu, Meiling Zhou, *Journal of Alloys and Compounds* **385** (2004) 288.
9. J.E. Alfonso, R. Garzón, and L.C. Moreno, *Physica B* **407** (2012) 4001.
10. C. Imawan), F. Solzbacher, H. Steffes, and E. Obermeier, *Sensors and Actuators B* **64** (2000) 193.
11. Z.A. Ansari, S.G. Ansari, T. Ko, J.-H. Oh. *Sensors and Actuators B* **87** (2002) 105.
12. P.F. Carcia and E. M. McCarron III, *Thin solid Films* **155** (1987) 53.
13. M. Shimoda, T. Hirata, K. Yagisawa, M. Okochi, and A. Yoshikawa *J. Mater. Sci. Lett.* **8** (1989) 1089.
14. R.J. Colton, A.M. Guzman, and J.W. Rabalais, *J. Appl. Phys.* **49** (1978)409.
15. S.S. Sunua, E. Prabhu, V. Jayaraman, K.I. Gnanasekar, T.K. Seshagiri, and T. Gnanasekaran, *Sensors and Actuators B* **101** (2004) 161.
16. Xingyi Deng et al., *Surface Science* **602** (2008) 1166.